

## Light propagation in a fishnet metamaterial

Carsten Rockstuhl,<sup>1,\*</sup> Christoph Menzel,<sup>1</sup> Thomas Paul,<sup>1</sup> Thomas Pertsch,<sup>2</sup> and Falk Lederer<sup>1</sup>

<sup>1</sup>*Institute of Condensed Matter Theory and Solid State Optics, Friedrich Schiller University Jena, 07743 Jena, Germany*

<sup>2</sup>*Institute of Applied Physics, Friedrich Schiller University Jena, 07743 Jena, Germany*

(Received 10 July 2008; published 2 October 2008)

We derive the dispersion relation of Bloch modes in a fishnet metamaterial in the optical frequency domain. The dependence of the longitudinal wave vector component on the transverse one and the frequency, which governs diffraction and dispersive spreading of localized light excitations, respectively, are analyzed. We show that this type of metamaterial exhibits an involved anisotropic behavior with diffraction changing the sign in passing even a zero diffraction point. For completeness we derive furthermore a formal angle-dependent effective refractive index which exhibits discontinuities. Thus we conclude that an effective refractive index tends to get meaningless and that only the dispersion relation predicts reliably light propagation in metamaterials. The results are double checked with those obtained from a retrieval algorithm based on angular resolved reflection/transmission data of a finite slab. Excellent agreement is observed.

DOI: [10.1103/PhysRevB.78.155102](https://doi.org/10.1103/PhysRevB.78.155102)

PACS number(s): 78.20.Ci, 41.20.Jb, 73.20.Mf, 75.30.Kz

Optical metamaterials (MMs) are a novel class of artificial matter.<sup>1</sup> They derive their properties primarily from an appropriately chosen geometry of the unit cells the MM is composed of. These unit cells are usually periodically arranged. Currently it may be anticipated that the most promising applications of MMs are the perfect lens<sup>2</sup> and the cloaking device.<sup>3</sup> Implementation of both concepts requires the understanding of light propagation in bulk rather than single layer MMs beyond normal incidence. It is generally assumed that the wavelength of the propagating field in MMs is much larger than the period of the arrangement and thus the MM is considered as an effectively homogeneous medium, which may be characterized by effective material parameters.<sup>4</sup> In doing this, the respective normal modes are assumed to be plane waves. However, it was pointed out recently that this assumption is critical in nowadays feasible MMs for the optical domain.<sup>5</sup> Violation of the above condition will entail that nonlocal effects will come into play evoking spatially dispersive behavior, in addition to the anticipated anisotropy. Because the exploitation of material properties not available in nature will open the realm of optical devices with unprecedented functionalities it is inevitable to completely understand the physics of light propagation in these materials. This concerns primarily the assignment of effective material parameters and includes the difference between *material* and *wave* parameters.

The simple example of a uniaxial crystal will help to state the issue. The arrangement of atoms, or the crystal's symmetry, together with the electronic properties yields a frequency-dependent dielectric tensor which is in this case an ellipsoid. The three principal axes, where two are equal, define the relevant dielectric functions  $\epsilon_i(\omega)$ , which represent the *material* parameters. Based on these two dielectric functions the dispersion relation of two unlike normal modes can be derived. For a fixed frequency this dispersion relation can be displayed as two isofrequency surfaces; the principal axes of which are defined by the *material* parameters. Fixing the direction of the wave vector, the intersection points with these surfaces provide the refractive indices  $n_{o,e}(\omega)$  of these two modes propagating in this particular direction, the *wave* parameters. Furthermore, the vector normal to these surfaces

defines the direction of energy flow. It is evident that for the extraordinary wave, *material* and *wave* parameters equal only along the principal axes whereas they coincide for the ordinary wave in all directions [ $\sqrt{\epsilon_1 \text{ or } 2}(\omega) = n_o(\omega)$ ]. Thus, it is clear that the assignment of a global effective refractive index is only meaningful if the isofrequency surface is a sphere. Finite beams are composed of a bundle of normal modes (finite angular spectrum), each of them pointing in a different direction. Thus the curvature of the isofrequency curves determines the strength and the sign of diffraction. In anisotropic, but homogeneous materials diffraction may vary in strength for the extraordinary beam but it is always normal. For the ordinary beam diffraction is invariant. The situation changes in periodic media as waveguide arrays<sup>6</sup> and photonic crystals,<sup>7</sup> where diffraction may become anomalous or can even be arrested, with the latter implying that the propagation of beams becomes possible which does not modify their profile. Thus, it can be anticipated that this behavior will likewise occur in MMs. It will be useful to keep this picture in mind in interpreting light propagation in bulk MMs and in designing MMs for applications.

To date there is no access to *material* parameters of MMs. This would require *ab initio* calculations for an electron gas, confined in the respective unit-cell geometry, in very large systems (in terms of solid-state theory) which exceeds by far the current CPU performance. Up to now the distinction between *material* and *wave* parameters did not play a significant role in the literature, except in a very recent paper,<sup>5</sup> because only normal incidence of a plane wave was considered. However, to translate the various MM concepts into practical devices, this limitation has to be lifted. For example, to realize a perfect lens  $n = -1$  is required for all transverse spatial frequencies. This sheds light on the image formation process using MM lenses. To date mostly an intuitive approach based on arguments of geometrical optics has been used to explain this perfect imaging. This approach is only useful if the material is effectively homogeneous and isotropic. Otherwise one has to resort to the dispersion relation (isofrequency curves) of Bloch modes (BMs) to derive the imaging properties based on wave optics arguments.

To date the most prominent numerical technique for disclosing the optical properties of MMs of finite thickness (calculation of the longitudinal wave vector component on the transverse one, assignment of effective parameters) is based on the inversion of the reflection ( $R$ ) and transmission ( $T$ ) coefficients of a plane wave at a slab, characterized by both an isotropic index and impedance.<sup>4</sup> Although the angular dependent spectral response of MMs was analyzed<sup>8</sup> this approach has been developed for normal incident fields only, or, associating the  $z$  axis with the principal propagation direction, for vanishing transverse wave vectors  $k_{x/y}$  thus circumventing the crucial issue of *wave vs material* parameters. As already pointed out genuine imaging applications require that the wave vector varies on the surface of a sphere (negative effective refractive index *independent* of  $k_{x/y}$ ). Thus the calculation of the longitudinal as a function of both transverse wave vector components (or the angle of incidence) in bulk MMs is still in order. In addition to these issues it was shown in Ref. 9 that another effect may even prevent the assignment of effective *wave* parameters. This will be the case if higher-order BMs are less or comparably damped as the fundamental BM. Overall the presence of such higher modes might cause the appearance of a series of anomalous refractive effects, as commonly known for photonic crystals.<sup>10</sup>

It is the aim of this contribution to shed some additional light on the above issues. The key questions to be answered are the following: (1) Can the excitation of higher-order BMs be suppressed? (2) If this is possible, which type of isofrequency curve, and thus refraction and diffraction properties, arises from the dispersion relation? (3) Is it possible and meaningful to introduce an effective index? (4) Do the results derived from the retrieval algorithm (valid for any thickness) and the dispersion relation (strictly valid only for infinite thickness) converge and which thicknesses are required for convergence? The first issue was already dealt with recently<sup>11</sup> and strategies have been put forward to avoid the excitation of higher-order BMs where it turned out that they can be fairly easily suppressed in the so-called fishnet structure. Upon technological considerations and experimental studies this structure has been found to be a promising MM with reasonable losses in the optical domain<sup>12–14</sup> and the potential for a bulk MM.<sup>15</sup> Thus it seems reasonable to focus our studies on this MM geometry. Although the MM studied will determine the particular form of the dispersion relation the general results of our investigations will hold for a wide class of MMs.

First, we shall derive the dispersion relation of BMs in this MM. These results are then compared with those retrieved from  $R$  and  $T$  for a finite MM slab at oblique incidence.<sup>20</sup> From both methods an effective refractive index will be derived and compared. This refractive index is no longer a global *wave* parameter which coincides with the *material* parameter but rather represents a *wave* parameter which varies with the angle of incidence. Our key result will be that light propagation in MMs can be fully understood by inspecting the dispersion relation whereas it seems to be meaningless to introduce an effective index the plane wave experiences. Even in cases where it can be defined it shows a complex behavior which is likely triggered by anisotropy

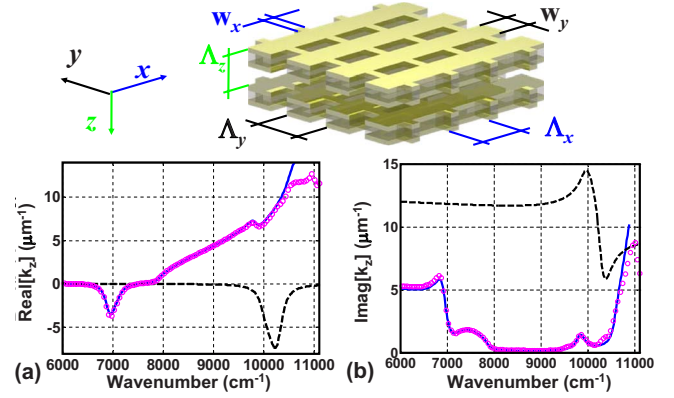


FIG. 1. (Color online) Geometry of the fishnet structure (top). The (a) real and (b) imaginary parts of the propagation constant  $k_z$  vs wave number are shown for the two lowest-order BMs and normal incidence. Zeroth order—blue solid line; first order—black dashed line. The results retrieved from  $R$  and  $T$  of a five-layer slab are shown by magenta circles.

and nonlocal effects in the MM. Thus it is impossible to characterize a MM of finite thickness by a single complex function of frequency. There are even situations where this effective index ceases to be meaningful at all because it becomes discontinuous. The structure is shown on top of Fig. 1.

The parameters are taken from the literature.<sup>12</sup> One fishnet layer consists of three material layers made of Ag-MgF<sub>2</sub>-Ag with thicknesses  $h_{\text{Ag}}=45$  nm and  $h_{\text{MgF}_2}=30$  nm. The wires that form the fishnet have a width of  $w_x=100$  nm and  $w_y=316$  nm. The lateral periods are  $\Lambda_x=\Lambda_y=600$  nm. The period in the  $z$  direction is  $\Lambda_z=200$  nm. The material between subsequent fishnets is air. For the calculation of the BM dispersion relation  $k_z=k_z(k_x, k_y, \bar{\nu})$  ( $\bar{\nu}=1/\lambda$  is the wave number) the transfer matrix of a layer containing a single unit cell in the propagation direction was employed. Enforcing Bloch periodic boundary conditions defines an eigenvalue problem which can be written as

$$\hat{\mathbf{T}}(k_x, k_y, \bar{\nu}) \mathbf{u}_m(k_x, k_y, \bar{\nu}) = e^{ik_{z,m}\Lambda_z} \mathbf{u}_m(k_x, k_y, \bar{\nu}), \quad (1)$$

with  $\mathbf{u}_m(k_x, k_y, \bar{\nu})$  being a vector comprising the tangential field components of the  $m$ th eigenmode in the angular and spectral Fourier spaces. The transfer matrix  $\hat{\mathbf{T}}(k_x, k_y, \bar{\nu})$  is indicated to depend on the wave number and the transversal wave vector components. The Floquet-Bloch ansatz for the field vector provides an algebraic eigenvalue problem that can be solved numerically with standard matrix routines. The longitudinal component of the wave vector  $k_{z,m}(k_x, k_y, \bar{\nu})$  as well as the BMs

$$\mathbf{E}_m(\mathbf{r}, t) = e^{i\mathbf{k}_m \cdot \mathbf{r}} \sum_{\mathbf{G}} \mathbf{E}_{\mathbf{G},m} e^{i\mathbf{G} \cdot \mathbf{r}} e^{-i\omega t}, \quad (2)$$

being represented as a superposition of plane waves,<sup>16</sup> can be calculated out of the eigensolutions of Eq. (1). The quantity  $\mathbf{G}$  denotes the reciprocal-lattice vector and  $m$  is attributed to the mode index. If the evolving field in the medium is dominated by a single mode and, in addition, if the expansion of

this dominating mode as given in Eq. (2) is dominated by a single plane wave, the material behaves effectively as homogenous to which effective properties can be attributed.<sup>17</sup> The major advantage of such a method that formulates the eigenvalue problem in the spectral Fourier space is the possibility to retain a potentially measured material dispersion and to retain only real valued frequencies. The propagation constant of the mode will be the only complex quantity, reflecting the absorptive nature of the material. The algorithm we used was described in detail in the literature.<sup>18</sup>

The dispersion relation assuming a plane-wave propagation inside the effective medium was also retrieved from  $R/T$  calculations of a finite MM slab consisting of 5 MM periods in  $z$  direction. Five MM periods turned out to be sufficient to ensure convergence between both approaches. The reflected and transmitted complex amplitudes were computed using the Fourier modal method (FMM).<sup>19</sup> On passing we note that the more equal the dispersion relations with both methods are, the better the assumption of an effective homogeneous medium is.

A Drude model was assumed in all simulations to describe the properties of Ag with the plasma frequency being  $\omega_{\text{Pla}} = 1.37 \times 10^{16} \text{ s}^{-1}$  and the collision frequency being  $\omega_{\text{Col}} = 8.5 \times 10^{13} \text{ s}^{-1}$ , respectively. The latter parameter is attributed to the damping of the electron-density oscillation. The parameter is also often termed in the literature as  $\Gamma$ , the damping. The refractive index of  $\text{MgF}_2$  was 1.38.

The dispersion relation  $k_z = k_z(0, 0, \bar{\nu})$  of the two lowest BMs is shown in Figs. 1(a) and 1(b). We restrict all considerations to the solutions with  $\Im k_z > 0$  which decay exponentially for  $z > 0$ . BMs with a dominant  $E_y$  component with respect to the unit cell in the  $y$  direction are shown. The zeroth and the first order BMs were selected from the infinite set as they possess the lowest imaginary part in the relevant domain. We note that in opposite to dielectric periodic media where for a fixed frequency a finite number of modes with real valued propagation constants, usually forming the band structure, and an infinite number of modes with imaginary valued propagation constants exist, such distinction is not possible for MM. Here all propagation constants are complex because of the intrinsic absorptive nature of the materials. Nevertheless, light propagation will be dominated by eigenmodes with the lowest imaginary part.

For the zeroth-order BM  $\Re k_z$  is negative between  $\bar{\nu} = 6300$  and  $7500 \text{ cm}^{-1}$ . It is the realm of negative refraction where  $\mathbf{k}$  and the Poynting vector  $\mathbf{S}$  are antiparallel. The first-order BM supports similar negative refraction at larger frequencies but cannot be excited for symmetry reasons. Its symmetry as compared to the fundamental mode can be inferred from Fig. 2, where the  $E_y$  component of the electric field of the eigenmodes is shown in the intersection plane between two subsequent layers (e.g., in a central plane between two fishnets). It can be seen that the field of the first-order BM has odd symmetry and cannot be excited from the outer region with a plane wave that would excite only modes with an even symmetry. Moreover, below  $\bar{\nu} = 10\,000 \text{ cm}^{-1}$  its imaginary part is much larger than that of the zeroth-order BM. Thus, an effective index, deduced from the zeroth-order BM,<sup>9</sup> can be formally introduced as  $n_{\text{Eff}}(0, 0, \bar{\nu}) = k_z(0, 0, \bar{\nu}) / 2\pi\bar{\nu}$  but provides no further insight.

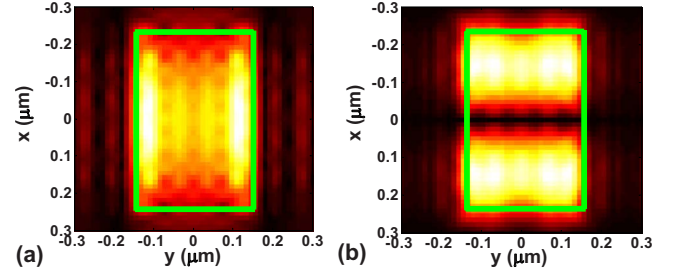


FIG. 2. (Color online) (a) Amplitude distribution of the  $y$  component of the electric field of the zeroth-order BM and the first-order BM in a plane between two fishnets.

For  $x$ -polarized BMs the dispersion relation for both lowest-order modes is monotonic. No negative refraction is observed. The chosen asymmetric unit cell causes the resonances in this polarization to occur at larger frequencies. This polarization is of no relevance to the present study and is not considered further. For comparison in Fig. 1  $k_z(0, 0, \bar{\nu})$  is also shown as retrieved from  $R/T$  calculations of a five-layer MM. Excellent agreement between the Bloch and the plane-wave approach can be recognized as long as the zeroth-order BM dominates.

Now we proceed with the case of oblique incidence. Figure 3(a) shows the dispersion relation (in this case the isofrequency surface) for the lowest-order BM as a function of  $k_x$  for  $k_y = 0$  and at  $\bar{\nu} = 6957 \text{ cm}^{-1}$ , where  $|\Re k_z|$  is largest at normal incidence. The values for  $k_x$  are restricted to  $k_x \leq 4.37 \mu\text{m}^{-1}$  corresponding to an incidence angle of  $90^\circ$ .

Most notably is the shape of  $\Re k_z(k_x)$ . If the material could be described by a global effective index this shape should be a circle (constant negative refraction and constant anomalous diffraction; the Poynting vectors point inward). It is evident that this is not the case here where diffraction properties change with increasing transverse spatial frequency because the curvature of the isofrequency curve varies. First, diffraction is anomalous, passing a domain of zero diffraction at the inflection point and showing ultimately normal diffraction for large spatial frequencies. The consequences for the imaging properties will be discussed elsewhere. The attenuation ( $\Im k_z$ ) varies less than  $\Re k_z$ . The change in the sign of the curvature basically implies also that the use of an anisotropic

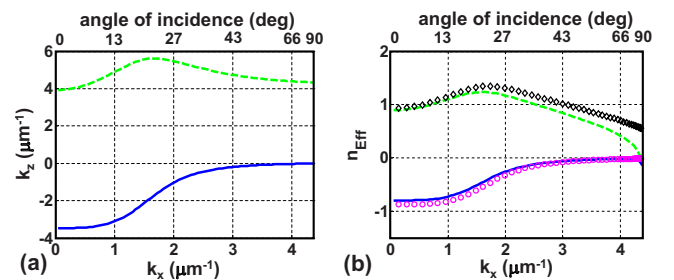


FIG. 3. (Color online) (a) Dispersion relation and (b) the derived effective index vs the angle of incidence of the lowest-order BM ( $k_y = 0$ ,  $\bar{\nu} = 6957 \text{ cm}^{-1}$ ; real part—blue solid line, imaginary part—green dashed line). In (b) the effective index retrieved from  $R$  and  $T$  of a finite slab is also shown (real part—magenta circles, imaginary part—black diamonds).



material model is not sufficient as then diffraction would have the same sign. Instead, the material shows a nonlocal response.

To clarify the issue whether the effective index is a meaningful quantity it may be formally introduced as

$$n_{\text{Eff}}(k_x, k_y, \bar{v}) = \pm \frac{1}{2\pi\bar{v}} \sqrt{k_x^2 + k_y^2 + k_z^2(k_x, k_y, \bar{v})}, \quad (3)$$

being of course a *wave* parameter as discussed earlier. This effective index can be calculated in two ways: by taking  $k_z$  either from the dispersion relation  $k_z(k_x, k_y, \bar{v})$ , yielding the index the Bloch wave encounters or retrieving it from  $R/T$  calculations of a homogenous isotropic slab of thickness  $d$ , yielding the index the plane wave in the effective medium encounters. The latter approach requires the retrieval algorithm to be extended toward oblique incidence. This procedure is outlined elsewhere<sup>20</sup> and leads to

$$dk_z = \cos^{-1} \left\{ \frac{\mu^c k_z^s (1 - R^2) + \mu^s k_z^c T^2}{T[\mu^c k_z^s (1 - R) + \mu^s k_z^c (1 + R)]} \right\} + 2m\pi, \quad (4)$$

where  $k_z^{s/c} = \sqrt{k_0^2 \epsilon^{s/c} \mu^{s/c} - k_x^2}$  are the wave vector components normal to the surface in the substrate (*s*)/cladding (*c*) with the respective permittivities  $\epsilon^{s/c}$  and permeabilities  $\mu^{s/c}$ . The results are displayed in Fig. 3(b). Some conclusions can be drawn. A variable (with angle of incidence) effective index  $n_{\text{Eff}}(k_x, 0, \bar{v})$  can be assigned to the MM but provides no simplification compared to the dispersion relation. The variation of this index hints clearly to anisotropy and potentially to spatial dispersion.<sup>21,22</sup> Spatial dispersion cannot be derived from the variation of the index with the transverse wave vector, but it is likely that the size of the structure compared to the wavelength leads to nonlocal effects.<sup>5</sup> Another interesting result is that the homogenization approach (effective medium, plane wave as normal modes) is fairly reliable and that higher-order BMs can be disregarded because the effective indices derived from both models almost coincide at least for the real part. The MM behaves like a metal for large angles of incidence. This can be physically well understood. The required strong dispersion of the magnetic properties stems from the excitation of an antisymmetric plasmon polariton resonance. Large angles of incidence impede the excitation of these modes. For a *y*-polarized wave at grazing incidence no adequate cut-wire pair exists in the unit cell and the MM acts as a diluted metal. The sign of the square root in Eq. (3) was chosen by enforcing  $\Im n_{\text{Eff}} > 0$ . No depolarization occurs.

To gain further insight into the angular resolved MM properties, the dispersion relation of the zeroth-order BM was calculated for some fixed, discrete values of  $k_x$  at  $k_y = 0$ . The results for  $k_x = 0, 1.75 \mu\text{m}^{-1}$ , and  $2.62 \mu\text{m}^{-1}$  are shown in Figs. 4(a) and 4(b).

The effective index of the BMs derived from Eq. (3) is shown in Figs. 4(c) and 4(d). For an increasing  $k_x$  the spectral domain of negative refraction is shifted toward higher frequencies. For comparison  $k_z$  and the effective index, as deduced from  $R$  and  $T$  of the finite slab, are likewise shown for  $k_x = 2.62 \mu\text{m}^{-1}$ . Perfect agreement is observed both for  $k_z$  and the index but an unprecedented feature appears at  $\bar{v}$

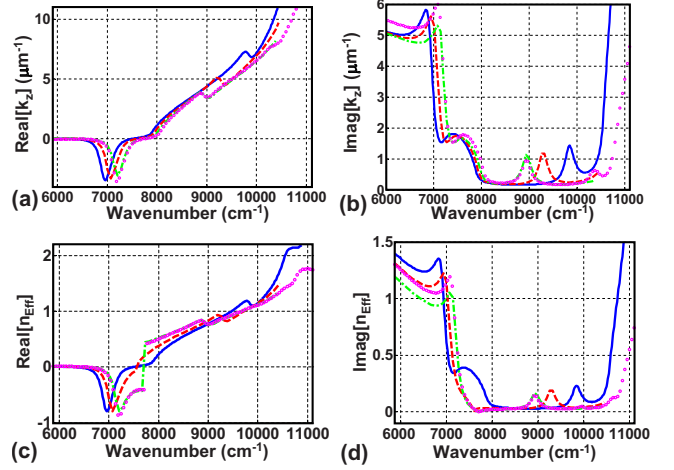


FIG. 4. (Color online) Longitudinal wave vector  $k_z$  [real part—(a), imaginary part—(b)] vs wave number for the lowest-order BM (blue solid line— $k_x=0$ , red dashed line— $k_x=1.75 \mu\text{m}^{-1}$ , green dashed-dotted line— $k_x=2.62 \mu\text{m}^{-1}$ ). The derived effective index is shown in (c) and (d).  $k_x=2.62 \mu\text{m}^{-1}$ . The figure shows also the longitudinal wave vector and the index of the plane wave retrieved from  $R$  and  $T$  of a finite slab (magenta circles).

$=7700 \text{ cm}^{-1}$ , where  $\Re n_{\text{Eff}}$  shows a discontinuity and  $\Im n_{\text{Eff}}$ , although hardly visible, shows a kink in both approaches used, whereas  $k_z$  is continuous. One might be inclined to eliminate this discontinuity by choosing the opposite sign for the square root in Eq. (3) at either lower or higher frequencies. But by doing so, the consequence is that  $\Re n_{\text{Eff}}$  is either positive or negative in the entire domain and  $\Im n_{\text{Eff}}$  is negative over an extended spectral domain. This would result in a discontinuity in  $\Re n_{\text{Eff}}(k_x)$  because the signs were unambiguously fixed at normal incidence.

However, this unphysical behavior concerns only the effective index of both BMs and plane waves and suggests that its introduction might be sometimes meaningless. But, even forgetting the above discontinuity for a moment, our results for oblique incidence have shown that the dispersion relations exhibit a shape different from those of isotropic, uni-, or biaxial media, even if only a single BM is relevant. Obviously it is in general not appropriate to describe the optical properties of a MM by such a global refractive index. Evidently the complexity of a nanostructured periodic material requires more rigorous means to describe the propagation of light. Theoretical optics predicts that this is the dispersion relation of normal modes. It relates all wave vector components with the frequency of light and is the only meaningful physical relation that has to be used. In all our calculations the results are in full agreement with the physical requirements, namely, the relevant wave vector component shows always a positive imaginary part and no discontinuities neither in the real nor in the imaginary part. The branch chosen exhibits the signature of negative refraction only over a narrow spectral domain. On the other hand, however, these studies show also that the homogenization procedure is quite reasonable because  $k_z = k_z(k_x, \bar{v})$  shows an almost identical behavior for the zeroth-order BM and the effective plane wave.

In conclusion, our studies provide a recipe how to de-

scribe light propagation in a MM. First, one has to derive the full dispersion relation  $k_z^m = k_z^m(k_x, k_x, \bar{v})$  of all BMs involved. Only if the fundamental BM ( $m=0$ ) exhibits much lower losses than the higher-order BMs reliable results can be derived. Thus this has to be ensured by MM design. Second, only if the dispersion relation provides a spherical isofrequency shape a global effective refractive index which is likewise a material parameter can be introduced. This holds likewise for isofrequency surfaces that compare to those of uni- or biaxial crystals. In this case two or three global indices might be meaningfully derived as material parameters. In all other cases the effective index provides no further information in addition to the dispersion relation, is a mere wave parameter, and can even behave unphysically. Third, comparing the results obtained from the dispersion relation with

those retrieved from  $R/T$  calculations yields two information, namely, how reliable a homogenization approach is and for which thickness the dispersion relation is applicable. This work is a first step to quantitatively analyze light propagation in MMs beyond normal incidence. It might pave the way to use MMs in applications as it allows to fully understand their properties.

#### ACKNOWLEDGMENTS

The authors acknowledge financial support from the German Federal Ministry of Education and Research (Metamat). Parts of computations were performed on the IBM p690 cluster JUMP of the JvN Forschungszentrum Jülich, Germany.

\*Corresponding author. carsten.rockstuhl@uni-jena.de

- <sup>1</sup>J. B. Pendry, A. J. Holden, D. J. Robbins, and W. J. Stewart, *IEEE Trans. Microwave Theory Tech.* **47**, 2075 (1999).
- <sup>2</sup>J. B. Pendry, *Phys. Rev. Lett.* **85**, 3966 (2000).
- <sup>3</sup>D. Schurig, J. J. Mock, B. J. Justice, S. A. Cummer, J. B. Pendry, A. F. Starr, and D. R. Smith, *Science* **314**, 977 (2006).
- <sup>4</sup>D. R. Smith, S. Schultz, P. Markoš, and C. M. Soukoulis, *Phys. Rev. B* **65**, 195104 (2002).
- <sup>5</sup>A. I. Cabuz, D. Felbacq, and D. Cassagne, *Phys. Rev. A* **77**, 013807 (2008).
- <sup>6</sup>T. Pertsch, P. Dannberg, W. Elflein, A. Bräuer, and F. Lederer, *Phys. Rev. Lett.* **83**, 4752 (1999).
- <sup>7</sup>R. Iliw, C. Etrich, U. Peschel, F. Lederer, M. Augustin, H.-J. Fuchs, D. Schelle, E.-B. Kley, S. Nolte, and A. Tünnermann, *Appl. Phys. Lett.* **85**, 5854 (2004).
- <sup>8</sup>F. Garwe, C. Rockstuhl, C. Etrich, U. Hübner, U. Bauerschäfer, F. Setzpfandt, M. Augustin, T. Pertsch, A. Tünnermann, and F. Lederer, *Appl. Phys. B: Lasers Opt.* **84**, 139 (2006).
- <sup>9</sup>D. Seetharamdoo, R. Sauleau, K. Mahdjoubi, and A. C. Tarot, *J. Appl. Phys.* **98**, 063505 (2005).
- <sup>10</sup>S. Foteinopoulou and C. M. Soukoulis, *Phys. Rev. B* **72**, 165112 (2005).

- <sup>11</sup>C. Rockstuhl, T. Paul, F. Lederer, T. Pertsch, T. Zentgraf, T. P. Meyrath, and H. Giessen, *Phys. Rev. B* **77**, 035126 (2008).
- <sup>12</sup>G. Dolling, C. Enkrich, M. Wegener, C. M. Soukoulis, and S. Linden, *Opt. Lett.* **31**, 1800 (2006).
- <sup>13</sup>S. Zhang, W. J. Fan, N. C. Panoiu, K. J. Malloy, R. M. Osgood, and S. R. J. Brueck, *Phys. Rev. Lett.* **95**, 137404 (2005).
- <sup>14</sup>U. K. Chettiar, A. V. Kildishev, H.-K. Yuan, W. Cai, S. Xiao, V. P. Drachev, and V. M. Shalaev, *Opt. Lett.* **32**, 1671 (2007).
- <sup>15</sup>G. Dolling, M. Wegener, and S. Linden, *Opt. Lett.* **32**, 551 (2007).
- <sup>16</sup>J. D. Joannopoulos, R. D. Maede, and J. N. Winn, *Photonic Crystals* (Princeton University Press, Princeton, NJ, 1995).
- <sup>17</sup>W. Śmigaj and B. Gralak, *Phys. Rev. B* **77**, 235445 (2008).
- <sup>18</sup>Z.-Y. Li and L.-L. Lin, *Phys. Rev. E* **67**, 046607 (2003).
- <sup>19</sup>L. Li, *J. Opt. Soc. Am. A* **14**, 2758 (1997).
- <sup>20</sup>C. Menzel, C. Rockstuhl, T. Paul, F. Lederer, and T. Pertsch, *Phys. Rev. B* **77**, 195328 (2008).
- <sup>21</sup>P. A. Belov, C. R. Simovski, and S. A. Tretyakov, *Phys. Rev. E* **67**, 056622 (2003).
- <sup>22</sup>C. R. Simovski and S. A. Tretyakov, *Phys. Rev. B* **75**, 195111 (2007).